Increased evolutionary rate in the Z-chromosome of sympatric and allopatric species of Morpho butterflies

Manuela López Villavicencio, Joséphine Ledamoisel, Riccardo Poloni, Céline Lopez-Roques, Vincent Debat, Violaine Llaurens

Increased evolutionary rate in the Z-chromosome of sympatric and allopatric species of *Morpho* butterflies.

Manuela López Villavicencio[1,2 *], Joséphine Ledamoisel[1,2], Riccardo Poloni[2], Céline Lopez-Roques[3], Vincent Debat[1,2], Violaine Llaurens[1,2],

1 Institut de Systématique, Evolution et Biodiversité (UMR 7205 CNRS/MNHN/SU/EPHE/UA), Muséum National d'Histoire Naturelle - CP50, 45 rue Buffon, 75005 PARIS, France
2 Centre Interdisciplinaire de Recherche en Biologie (UMR 7241 CNRS/INSERM/Collège de France) 11, place Marcelin Berthelot, 75005 Paris, France
3 GeT-PlaGe, Bât G2, INRAe, 24 chemin de borde rouge - Auzeville, CS 52627, 31326 CASTANET-TOLOSAN Cedex, France

*** Author for Correspondence: mlopez@mnhn.fr**

Abstract

Divergent evolution of genomes among closely related species is shaped by both neutral processes and ecological forces, such as local adaptation and reinforcement. These factors can drive accelerated evolution of sex chromosomes relative to autosomes. Comparative genomic analyses between allopatric and sympatric species with overlapping or divergent ecological niches offer insights into reinforcement and ecological specialization on genome evolution. In the butterfly genus *Morpho*, several species coexist in sympatry, with specialization across forest strata and temporal niches. We analyzed the genomes of eight *Morpho* species, along with previously published genomes of three others, to compare chromosomal rearrangements and signs of positive selection in the Z chromosome *vs* autosomes. We found extensive chromosomal rearrangements in Z chromosome, particularly in sympatric species with similar ecological niches, suggesting a role for inversions in restricting gene flow at a postzygotic level. Z-linked genes also exhibited significantly higher dN/dS ratios than autosomal genes across the genus, with pronounced differences in closely related species living in sympatry. Additionally, we examined the evolution of eight circadian clock genes, detecting positive selection in Period, located on the Z chromosome. Our findings suggest that the Z chromosome evolves more rapidly than autosomes, particularly among closely related species, raising questions about its role in pre- and post-zygotic isolation mechanisms.

Keywords

Fast Z, Inversion, Lepidoptera, Speciation, Reproductive isolation

Significance statement

Using comparative genomics, we investigate the evolutionary dynamics in sex chromosomes in sympatric butterfly species of the genus *Morpho*, and detected increased level of divergence in both coding sequences and structural variants. We found significantly enhanced signals of positive selection in genes located on the sex chromosome Z as compared to the autosomes, in particular on the circadian gene *Period*, that may be involved in the adaptation to divergence diel niche in

sympatric species. Our results therefore raise new questions on the role of the sex chromosome Z in ecological niche differentiation and/or reinforcement of barriers to gene flow.

Introduction

Sex chromosomes have been observed to undergo accelerated rates of sequence evolution compared to autosomes (Sackton et al., 2014), a phenomenon commonly known as fast-X or fast-Z evolution (Charlesworth et al., 1987; Vicoso and Charlesworth, 2006). The faster evolution of sex chromosomes has been observed in different groups with ZW system as some birds, snakes, and the salmon louse *Lepeophtheirus salmonis* (Irwin, 2018; Mank et al., 2009; Mongue and Baird, 2023; Vicoso et al., 2013; Wright et al., 2015), although contradictory trends have also been observed (*e.g.* in Lepidoptera, Rousselle et al. (2016)).

Within species, faster evolution of sex chromosomes can result from the effect of genetic drift limiting the purge of deleterious mutations when the effective populations size is reduced. For every mating pair, there are indeed four copies of autosomal genes and only three copies of X or Z-linked genes. Consequently, the effective population size (Ne) for X or Z sex chromosomes is reduced as compared to the autosomes ($3/4N_e$). Such reduced N_e may limit the loss of slightly deleterious mutations within each species, and may also enhance the probability of fixing adaptive mutations (Johnson and Lachance, 2012; Vicoso and Charlesworth, 2006). Between species the fixation of divergent mutations under positive selection on the sex chromosomes X and Z may be further promoted by the hemizygosity of X and Z chromosomes in XY males and ZW females respectively. Hemizygozysity directly exposes rare advantageous recessive alleles to selection and leads to greater rates of fixation compared to rare autosomal alleles that are sheltered in heterozygotes (Johnson and Lachance, 2012). Positive selection has been suggested to promote faster-X and Z evolution in mammals, *Drosophila* (XX/XY sex-determination system), but also in lepidoptera (ZW/ZZ sex-determination system), like the silkmoth *Bombyx huttoni*, the moth *Manduca sexta* and the butterfly *Danaus plexippus* (Meisel and Connallon, 2013; Mongue et al., 2022; Sackton et al., 2014). In the Crambidae moth *Ostrinia nubilalis*, a presumed 4 Mb inversion in the Z chromosome appears to increase the accumulation of ecologically adaptive alleles and genetic differentiation Wadsworth et al. (2015). Inversions capturing adaptive variants located on the sex chromosomes are thus expected to disproportionately contribute to the evolution of local adaptation (Connallon et al., 2018). Different Z-located inversions may thus be observed in closely-related species evolving in different ecological niches.

In sympatric or parapatric species, divergence in the sex chromosomes may also be further enhanced by their role in pre- and post-mating isolation (Payseur et al., 2018). Introgression in the sex chromosomes has been shown to be reduced as compared to the autosomes (Fraïsse and Sachdeva, 2021; Schilthuizen et al., 2011). For instance, in sister-species of *Ishnura* damselflies with overlapping geographic ranges, the levels of introgression was shown reduced in the X chromosome, as compared to the autosomes (Swaegers et al., 2022). Furthermore, comparisons between species of passerine birds revealed that structural variants were more prevalent on the Z-chromosomes as compared to the autosomes (Hooper and Price, 2017) and were more likely to be fixed between species pairs with overlapping geographic distribution, suggesting an effect of reinforcement on the fixation of divergent structural variants. Finally, genes involved in sexual dimorphism and mate preferences are also frequently found on the sex chromosomes and may also contribute to pre-mating isolation: for instance, in closely-related species of *Ficedula* flycatchers, loci controlling plumage divergence and preference for plumage coloration are located on the Z-chromosomes, and are likely to enhance pre-mating barriers (Sæther et al., 2007). Sex chromosomes may thus play a prominent role in the evolution of reproductive isolation in closely-related species living in sympatry. In Lepidoptera, evidence for a significant role of the Z-chromosome in reinforcement has been reported. In a pair of sister-species of *Colias* butterflies with overlapping geographic range, increased genetic divergence in the Z-chromosomes as compared to the autosomes was observed. Moreover, loci controlling for divergent coloration in males are located on the Z-chromosome, suggesting a key role

of the Z-chromosome in the pre-zygotic barrier to gene flow in these species (Ficarrotta et al., 2022).

Here, we focus on the genomic divergence between species of *Morpho* butterflies, where multiple species currently co-exist in sympatry in the Amazonian rainforest (Blandin and Purser, 2013). In the genus *Morpho*, sympatric species show divergence in (1) flight height, with specialisation in the canopy *vs.* understory microhabitat (Le Roy et al., 2021a) and in (2) flight time (Le Roy et al., 2021b). Males from some species only fly early in the morning, while males from other species typically patrol at noon (Gayman et al., 2016). Such specialisation into different forest strata and/or temporal niches likely contributes to the co-existence of these closely-related species in sympatry and may also have played a role in the speciation process itself. In the noctuid moth *Spodoptera frugiperda*, populations specialised on different host-plants diverge in the timing of mating, and the gene *vrille*, involved in the control of the circadian clock, was shown to diverge between these species (Hänniger et al., 2017). The evolution of circadian genes may thus be involved in the divergence of temporal niches in *Morpho* butterflies, therefore enhancing pre-zygotic barrier to gene flow in sympatric species. Interestingly, in Lepidoptera, some genes involved in the regulation of circadian behaviour are sex-linked: for instance, the gene *Period*, responsible for diurnal or nocturnal activity in some butterflies and moths or the gene *Clock*, involved in the photoperiodic response and migration in the Monarch buterfly, are both located on the Z-chromosome (Gotter et al., 1999; Iiams et al., 2019; Wang et al., 2023). We thus aimed at comparing the evolution of genomic divergence between the Z chromosomes and the autosomes in sympatric *vs.* allopatric species of *Morpho*, and specifically test for signals of positive selection.

We report the sequencing, assembly and annotation of the genomes of eight species from the genus *Morpho* based on long read data for individual butterflies which are near chromosome complete. We then used these new genome assemblies, as well as the previously published genomes of three other *Morpho* species (Bastide et al., 2023) to perform comparative genomic analyses in 11 out of the 30 species of the genus *Morpho*. We specifically compare the evolution of the Z-chromosome *vs.* the autosomes, in sympatric and allopatric species, specialized in different ecological niches: we investigate inversions and ratio of synonym *vs.* non-synonym variations in the region of the Z-chromosome *vs.* the autosomes. We also investigate the location and evolution of eight genes known to regulate circadian activities in other Lepidoptera (*Clock, Cycle, Period, Timeless, Cry1, Cry2, Vrille and PDP1*) (Brady et al., 2021; Reppert, 2006), and specifically test for signature of positive selection on these genes, potentially involved in pre-zygotic isolation.

Results

Nuclear and mitochondrial genome assembly

For the eight genomes analyzed here, GenomeScope analyses suggested very high levels of heterozygosity going from 1.01% in *Morpho granadensis* to 3.38% for *M. menelaus* (S1.The assemblies produced by Hifiasm showed nuclear genome sizes of the *Morpho* species ranging from 375 to 514Mb (see Table 1). Consistent with other Lepidoptera and with the known genomes of other *Morpho* species. In all cases, BUSCO results showed a very high level of duplicated sequences, when the assembly was performed using the option -l0 (no purge) in Hifiasm and in most cases, we had to use the option -l3 (most aggressive purge). The BUSCO values then showed low levels of duplicates in the assemblies for *M. telemachus* (for the blue and gold morphs), *M. amathonte* and *M. granadensis*. In contrast, *M. hecuba*, *M. menelaus*, *M. eugenia* and *M. marcus* genome assemblies still showed high levels of duplicates despite the use of the l3 option and needed to be further purged using Purge_dups. In the case of *M. rhetenor*, the best assembly was obtained without purging in Hifiasm, but with the use of Purge_dups. Final BUSCO results are shown in the Fig. S1 a). Mitochondrial genomes assembled using Rebaler presented similar sizes to the previously assembled genomes of other *Morpho* species (Bastide et al., 2023). For the nine individuals sequenced here, the Rebaler software detected mitochondrial genomes, with sizes ranging from 13,469 bp for the grey morph of *M. telemachus* to 16,173 bp in *M. amathonte*.

	Heterozygosity (%)	Genome size	Total contigs	N50	Content of RE (%)
M. rhetenor	2.50	375.99Mb	65	13Mb	40.43
M. hecuba	1.71	448.02Mb	64	14Mb	49.52
M. amathonte	1.69	467.10Mb	81	13Mb	49.89
M. menelaus	3.38	412.92Mb	34	12Mb	41.46
M. granadensis	1.00	448.90Mb	100	12Mb	49.95
M. eugenia	2.53	514.40Mb	34	11Mb	53.43
M. marcus	2.36	457.33Mb	56	11Mb	47.92
M. telemachus gold	1.19	447.12Mb	62	14Mb	51.14
M. telemachus blue	1.11	449.72Mb	68	13Mb	50.09

Table 1. Heterozygosity, Genome size, Number of contigs, N50 and percentage of the genome covered by repetitive elements (RE) for the assemblies of eight *Morpho* species. Assemblies were performed using Hifiasm and were purged using Purge_dups when needed based on BUSCO results on the assembly. The number of total contigs corresponds to the number of contigs obtained after assembly and before any further treatment of the assemblies.

Genome annotation

The use of RepeatMasker and RepeatModeler produced results similar to previous ones on other *Morpho* genomes (Bastide et al., 2023): repeated elements account for 40% to 53% of the genomes of the nine *Morpho* species sequenced here (Table 1) By re-annotating the three previously published *Morpho* genomes (*M. helenor*, *M. achilles* and *M. deidamia*), we found significantly more genes predicted and better proteome BUSCO scores using BRAKER2 than with the previous methodology using Maker v2.31.10 (Bastide et al., 2023). Between 18,159 and 21,017 protein coding genes were annotated within each genome of most *Morpho* species studied here (see table S3). These values fall within the range observed in other Nymphalidae species, as *Euphydryas editha* (Tunstrom et al., 2022). For *M. helenor*, the annotation pipeline predicted 29,734 complete genes, a number significantly higher than those for other *Morpho* species and Nymphalidae in general. The use of ContScout revealed that the excess of annotated genes resulted from a high number of foreign sequences, principally from bacteria (see Table S3). All these contaminations were removed from the assembly and were excluded from further analyses.

Phylogenetic relationships between *Morpho* species

We inferred the phylogenetic relationships among samples using 8780 single-copy orthologs detected in all 12 available genomes of *Morpho*, using IQTree and ModelFinder. This whole-genome phylogeny is consistent with the published phylogeny of the group, inferred from mitochondrial and nuclear genes (Chazot et al., 2021, 2016). All the canopy species form a single monophyletic clade while understory species are distributed in two clades (Fig. 1). The divergence between the "blue" and the "gold" morphs within the species *M. telemachus* is very low (dxy = 0.02) and the branch much shorter than those separating sister species like *M.helenor* and *M.achilles*, or *M.eugenia* and *M.marcus*. This confirms that these two syntopic colour morphs belong, in fact, to the same polymorphic species.

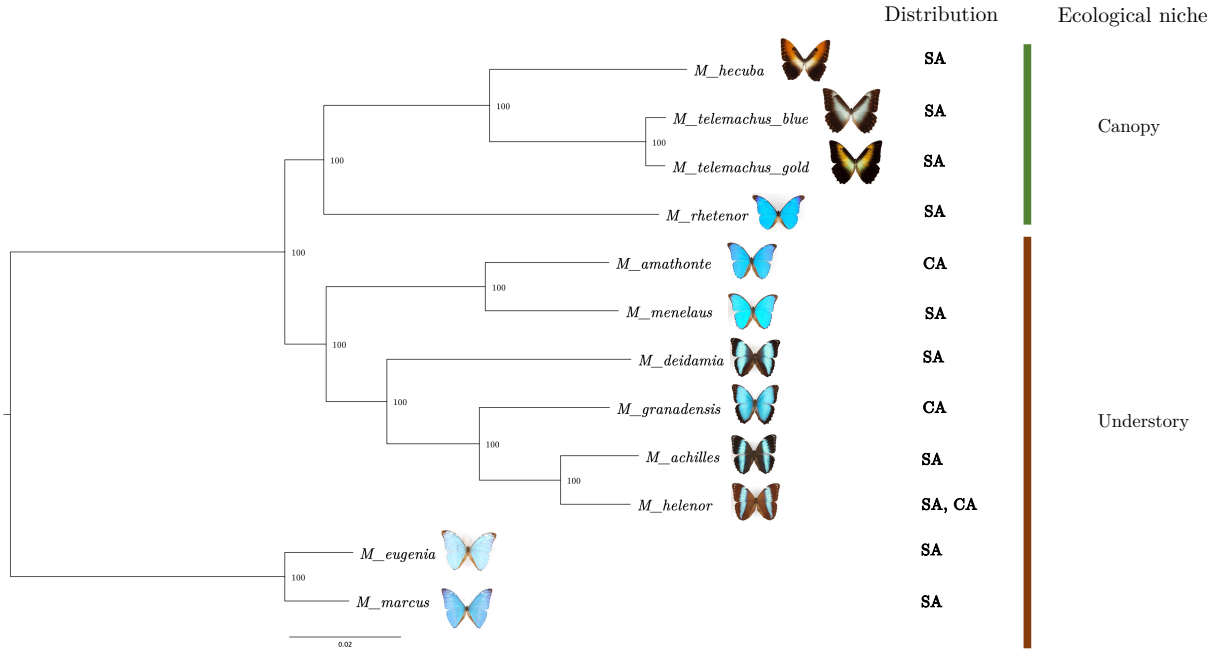

Figure 1. Phylogenetic relationships between the 12 *Morpho* samples inferred using IQ-TREE together with Q.mammal+F+I+R8 substitution model and ultrafast bootstrap with 1000 replicates. Analyses were performed with a supermatrix from 8780 single-copy orthologs extracted with OrthoFinder and found in all the samples. Bootstrap values are displayed next to the nodes. Additionally, the ecological niche (canopy or understory) and species distribution (South America - SA or Central America - CA) are indicated.

Synteny and detection of chromosomal rearrangements between *Morpho* genomes

After assembling the different contigs within each *Morpho* species, we identified a contig that shares synteny with the Z contig previously identified in *M. helenor* (Bastide et al., 2023). The size of this contig varied across species, ranging from approximately 18 to 25 Mb. Notably, it was the largest contig within each assembly, for all species except *M. marcus* and *M. eugenia* (Fig. S2). Although our assemblies did not reach chromosome-level resolution, the size of this contig was similar to the Z chromosome size observed in related species with high-quality chromosome-level assemblies, such as *Maniola jurtina* (17 Mb) (Lohse et al., 2021), *Pararge aegeria* (27 Mb https://www.darwintreeoflife.org/project-resources/), or *Bicyclus anynana* (24 Mb) (Saccheri et al., 2023). This observation suggests that the identified Z contig may closely approximate the true Z chromosome size in *Morpho*.

D-genies whole-genome paired alignments showed strong synteny in all autosomes across the majority of closely-related species (Fig. S3). On the other hand, they revealed inversions in the Z contig among pairs of closely-related species (Fig. S3): three among the seven paired comparisons unveiled variable-sized inversions (Fig 2). Further analyses using SyRI revealed, for the species living in the understory, three inversions measuring a total of more than 7Mb positioned at the tips of the Z contig among *M. granadensis* and *M. helenor* and three inversions measuring together 2Mb between *M. helenor* and *M. achilles* (Fig 2 subfigure a). Within the canopy clade, a 2.5 Mb inversion was identified between *M. telemachus* and *M. hecuba* (Fig 2, subfigure b). While D-genies whole-genome comparisons uncovered two small inversions between *M. telemachus* and *M. rhetenor* (see S3) these were not observed in the paired comparisons conducted with SyRI (see Fig 2 subfigure b). SyRI plots between these two species revealed lower synteny in the Z contig compared to other species pairs. Additionally, the contig in *M. rhetenor* showing the highest synteny to the Z contig in *M. telemachus* was much smaller for *M. rhetenor* suggesting that the regions capturing the inversions observed in whole-genome comparisons were not included when contigs were isolated for analysis with SyRI. Comparisons also showed two pairs of closely-related species without any inversions and with a very high synteny level along the entire Z contig: *M. menelaus* vs *M. amathonte* and *M. eugenia* vs *M. marcus* (Fig 2 subfigures c and d). Nevertheless, for these species, small inversions were found in the autosomes. The comparison between *M. menelaus* vs *M. amathonte* revealed a 280000 bp inversion in the contig ptg000019l (Fig. S2 a) while for *M. eugenia* vs *M. marcus* small inversions between 392980bp and 431811bp were found when comparing the contig ptg000027l of *M. eugenia vs* the equivalent contig ptg000011l of *M. marcus*. We also found inversions of between 714789bp and 895465bp when comparing contigs ptg000024l of *M. eugenia* and the equivalent contig ptg000013l of *M. marcus* (Fig. S2 b) and c) respectively). Overall, our results revealed a higher frequency of larger inversions on the Z contig compared to the autosomes. However, note that we restricted our inversion detection to contigs larger than 10 Mb (or 5 Mb in the case of *M. hecuba*, see Materials and Methods), preventing us to observe inversions occurring in smaller-sized autosomal contigs.

Higher dN/dS on the Z chromosome and signatures of positive selection in circadian genes

The *dN/dS* ratio (ω) of all orthologous genes located on the Z contig (148 genes) *vs.* the autosomal contigs (8209 genes) was first measured throughout the 12 *Morpho* species. Using the gapless ortholog alignements, we found that the genes located on the Z contig have a significantly higher ω than the genes located on the autosomal contigs (Wilcoxon test: $p - value = 0.0004996$, Fig 3 a). The same trend is found when calculating the ω ratio using the raw ortholog alignments, Fig S4. Because the number of genes on the Z contig was much lower than the genes located on the autosomes, we performed permutation tests. These binomial tests showed that the p-values calculated are significantly lower than the 0.05 threshold (p-value<2.2E-16 for both distributions, raw et gapless orthologs), confirming that the ω ratio of the genes found on the Z contigs is indeed higher than the ω ratio of the genes found on the autosomal contigs (Fig. S5).

To test for divergent evolution in species evolving in the canopy vs. the understory, we used a

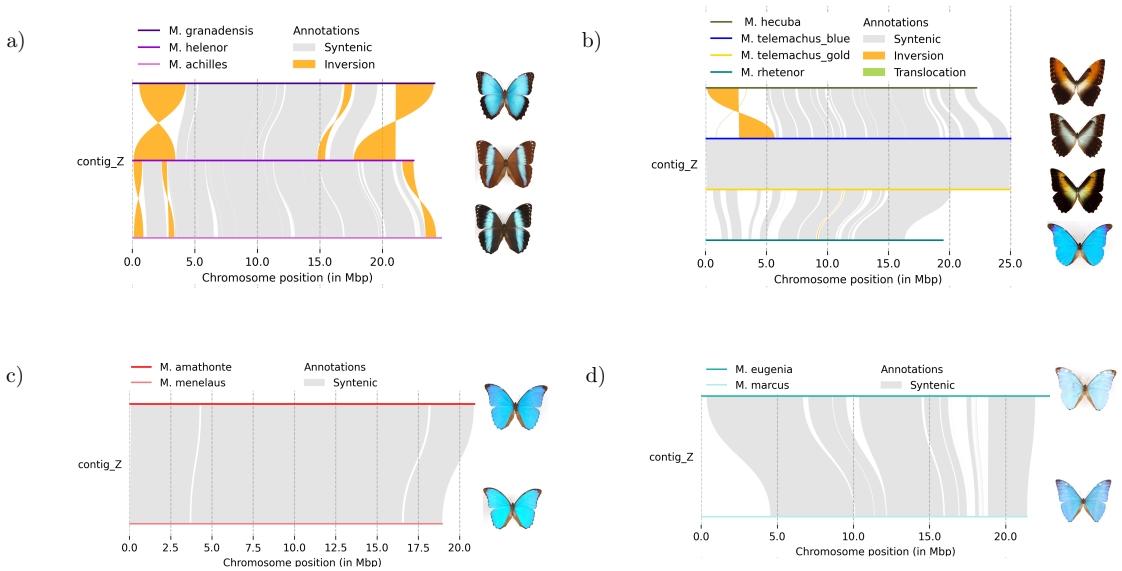

Figure 2. Paired comparisons of the region corresponding to the Z contig between closely-related *Morpho* species. The species compared are a) understory species *M. granadensis* and sister species *M. helenor* and *M. achilles* b) all the species belonging to the canopy clade c) understory sister species *M. amathonte* and *M. menelaus* d) basal clade *M. eugenia* and *M. marcus*. Inversions are visible in dark yellow and syntenic regions in light gray

clade model to compare the evolutionary rates of genes located on the Z chromosome and autosomes between species from the canopy and those from the understory. This test revealed that approximately 4.6% of the genes on the autosomes exhibited significant differences in evolutionary rates between the canopy and understory clades, while only 0.68% of the genes on the Z chromosome showed such significant differences. A Z-test for proportions showed a significant difference between the autosomal and Z chromosome groups (Z-value: 2.27, p-value: 0.02) (Fig. S6). This analysis focused on the genes shared by both clades and did not detect a prominent role of Z-linked genes in the divergent adaptation to different habitats. We then analysed of species within each clade separately (canopy or understory), allowing to study clade-specific genes as well. We estimated differences in the evolutionary rates between autosomes and the Z chromosome using the M0 model in codeml. This analysis revealed significant differences in the mean dN/dS ratio between genes located on the autosomes and those on the Z chromosome, but the direction of these differences was opposite between the two groups. For the eight understory species, the mean ω was significantly higher for genes on the Z chromosome than for those on the autosomes (Wilcoxon permutation test: Z = -2.58, p-value = 0.0098, Fig. S7). In the canopy species however, the mean ω was higher for genes on the autosomes than for those on the Z chromosome (Wilcoxon permutation test: Z = -5.14, p-value = 1e-05). Nevertheless, in this group, we only had three species, therefore questioning the robustness of this last result. These clade-specific analyses suggest that adaptation to the micro-habitats is probably not the main driver of the enhanced dN/dS ratio in the Z-contig as compared to the autosomes, detected at the genus scale.

We then tested whether the difference between the gene evolution in the Z-contigs and the autosomal contigs was more prevalent in closely-related species living in sympatry, in line with putative effect of reinforcement of species barriers. We thus computed dN/dS ratio for different species pairs using the YN00 program. These pairwaise analyses revealed significant differences in mean ω between autosomes and chromosome Z in all comparisons involving pairs of canopy species and pairs of closely related species from the understory (*i.e.* pairs belonging to the *granadensis achilles helenor deidamia* clade), regardless of whether they were sympatric or allopatric (Fig 3 b). In contrast, no significant differences in mean ω between autosomes and chromosome Z were found for the basal clade pair (*M. marcus* and *M. eugenia*), the two closely related understory species *M. amathonte* and *M. menelaus*, or in pairs involving species from different ecological habitats (Fig. 3 b). Heterospecific interactions in sympatry are thus not specifically associated with increased differences in the evolution of genes located in the Z-contigs vs. the autosomes, but this difference observed at the genus scale, is probably mostly driven by divergent evolution of the Z-chromosome between closely-related species.

Positive selection tests were also specifically computed on eight circadian genes. The random site models implemented in PAML applied to our 12 *Morpho* samples did not reveal any signal of positive selection on any of the eight tested circadian genes (Table S4). However, using a branch site model, evidence of positive selection was found in one of these genes when comparing the canopy *vs.* understory species: a significant signature of positive selection in the canopy lineage was found in *Period*, located on the Z contig ($p - value = 0.03$, see Table S5). Such positive selection detected on sites where amino acids are different between the canopy and the understory species suggests that different selective pressures may affect the evolution of the *Period* gene in the two micro-habitats (Fig 4).

Introgression among sympatric species

To test for gene flow among *M. granadensis* and *M. helenor* living in sympatry in Central America, we carried out ABBA-BABA tests, comparing the amount of shared genetic variation between these two species and the closely related species *M. achilles* and *M. deidamia*. All contigs show D-statistics values close to 0 ($-0.10 < D < -0.03$), without any significantly departure from the mean (Z score < 3).

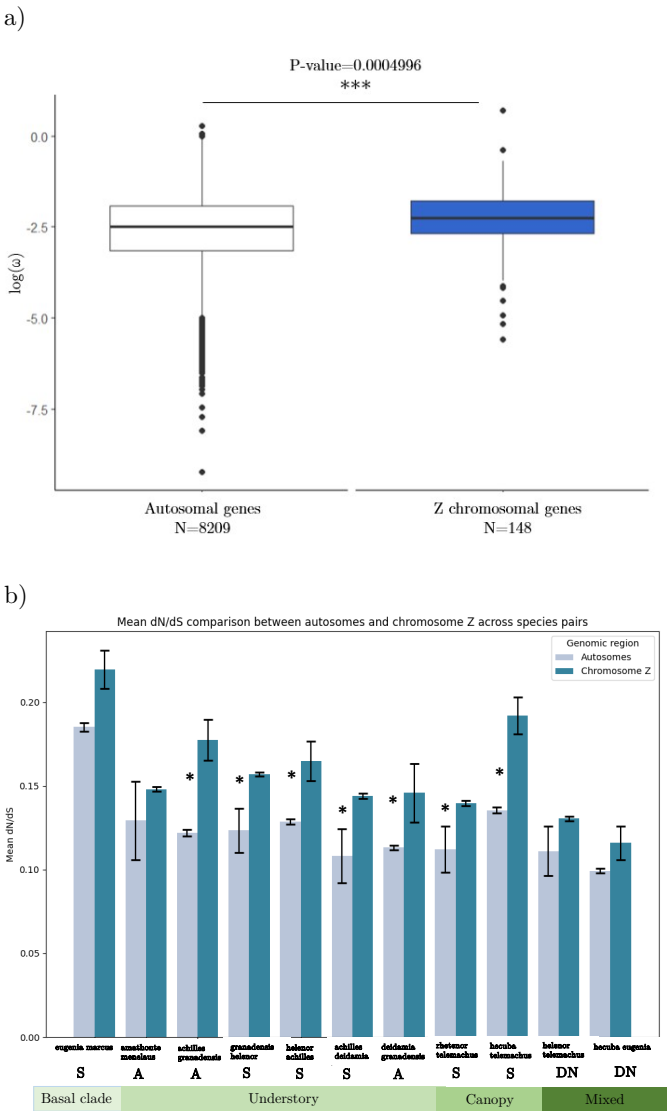

Figure 3. Comparison of the *dN/dS* values measured for a) the 8357 genes located in either the autosomal contigs (in white) or the Z contig (in blue). The ω ratio values were computed using the one-ratio model implemented in PAML on gapless ortholog alignments, and are represented in logarithmic scale. b) Mean ω for autosomes and chromosome Z estimated using the YN00 program with the method of Yang and Nielsen for pairwise comparison. Different pairwise comparisons were made: between the two species from the basal clade, between species from the understory (species pairs found in sympatry (S) and allopatry (A), between species from the canopy and finally, mixed comparisons between species from different ecological niches: canopy *vs* understory (DN). Asterisk represents a significant difference in the ω value between autosomes and the chromosome Z ($p < .05$)

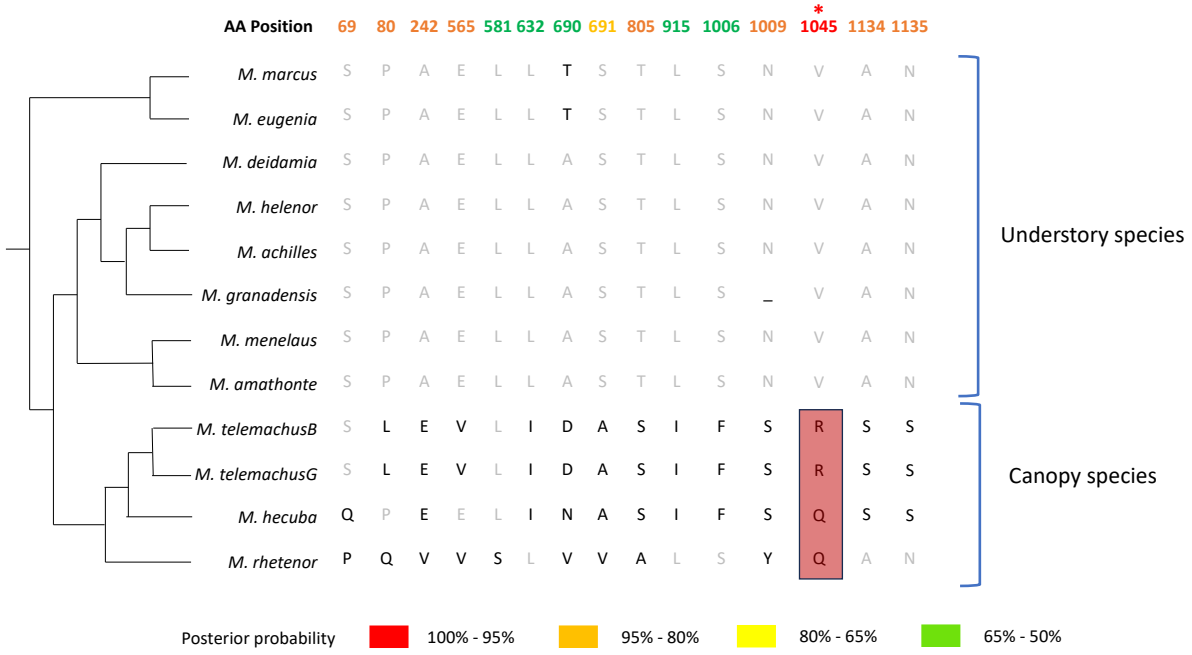

Figure 4. Partial amino acid alignment of the gene *Period* in *Morpho* species from the understory and the canopy, showing only the amino acids with a signature of positive selection using the branch site model in the PamL analysis. The position of these amino acids along the *Period* protein gene are indicated above in color. The values of the posterior probability associated with each site are indicated in colors, red indicating the highest probability (95 - 100%) and green the lowest probability (50 - 65%).

Discussion

By comparing the genomes of 11 *Morpho* species, our study suggests an increased evolutionary rate of the Z sex contig relative to the autosomal contigs in this genus. We specifically found an elevated dN/dS ratio in this contig as compared to the autosomal contigs. The prevalence of inversions was also much higher in the Z contigs, especially between closely-related species sharing a similar ecological niche and similar flight hours in sympatry. We discuss below the demographic and ecological factors that may have led to this accelerated divergence of the Z-chromosome as compared to the autosomes.

Prevalent inversions in the Z chromosome of sympatric sister-species

In the genus *Morpho*, we found that big inversions of more than 1Mb on the Z chromosome were more common among closely-related species coexisting in sympatry, particularly between species with overlapping temporal niches, such as the canopy species *M. hecuba* and *M. telemachus*, or the understory sister-species *M. achilles* and *M. helenor* and *M. granadensis* and *M. helenor* (Le Roy et al., 2021b)(Gayman et al., 2016). Conversely, big inversions were not observed in comparisons between closely related sympatric species with non-overlapping temporal niches, such as the basal sister-species *M. eugenia* (which flies very early in the morning around 6:00 AM) and *M. marcus* (which flies much later around 9:00 AM) (Gayman et al., 2016), or between species found in allopatry, such as *M. amathonte* and *M. menelaus*. Chromosomal inversions have long been

acknowledged as a crucial mechanism acting as barrier to gene exchange, ultimately driving speciation (Noor et al., 2001). Our results are thus consistent with a putative role of inversions located on the Z chromosome in the speciation and/or reinforcement process in the butterfly genus *Morpho*. Structural variations within each species now need to be investigated to test for fixation within species and better characterize the selective regime acting on the inversions within species.

The effect of the Z chromosome as a barrier to gene flow should be also reflected in the introgression rates between sympatric and closely related species, similarly to what has been found in *Heliconius* butterflies (Martin et al., 2013). Here, we did not detect any significant introgression between the closely-related species *M. helenor* and *M. granadensis* neither in the Z-contig nor in the autosomal contigs. Given the distribution of the species studied, we could only test for introgression between *M. helenor* and *M. granadensis*, whose distribution partially overlap in Central America. But the sister-species of *M. helenor*, namely *M. achilles*, also has an overlapping geographic range with *M. helenor* in the amazonian basin, so that gene flow could occur both between *M. helenor* and *M. granadensis* in Central America and between *M. helenor* and *M. achilles* in South America, strongly limiting the power of the ABBA/BABA test. Investigating the intra-specific genetic variability within these three species throughout South and Central America will allow clarifying the level of introgression in the Z vs. autosomal contigs in the future.

Evolution of circadian genes

Since *Morpho* species living in sympatry display temporal segregation throughout the day (Le Roy et al., 2021b), we specifically examined signatures of selection in various circadian genes previously documented in other Lepidoptera (Merlin and Reppert, 2009). We found evidence of positive selection on specific sites within the *Period* gene, that is located on the Z chromosome in *Morpho*, as well as in all Lepidoptera species studied so far (Sandrelli et al., 2008). Among circadian genes, *Period* has been suggested to be involved in sympatric speciation across multiple taxa: variation in the amino-acid sequence of the *Period* protein, and variation in the regulatory regions of the *Period* gene have been shown to be involved in allochrony, *i.e.* differences in breeding time among conspecific individuals, that may facilitate speciation (Taylor and Friesen, 2017). Experiments involving transgenic flies conducted by (Tauber et al., 2003) indicated that *Period* played a role in speciation in both *D. melanogaster* and *D. pseudoobscura*, by exerting control over the precise timing of mating behavior (Tauber et al., 2003). In the fly *Bactrocera cucurbitae*, *Period* was found to contribute to pre-mating isolation in two lines with distinct circadian periods, one short and one long (Miyatake et al., 2002).

In Lepidoptera, differences in diel activity are assumed to contribute to prezygotic reproductive isolation, as evidenced by the temporal segregation across 400 co-occurring species of Neotropical Hesperiidae (Devries et al., 2008). Nevertheless, the role of circadian genes in regulating these differences or their putative role in speciation has been scarcely studied, except in a few moth species. In *Spodoptera frugiperda*, the circadian gene *vrille* was found responsible for allochronic differentiation in the mating time of two different strains, by acting as a pre-mating barrier (Hänniger et al., 2017). In the moth *Plutella xylostella*, the CRISPR/Cas9-mediated genome editing to knockout the *Period* gene changed circadian rhythms patterns in pupal eclosion, mating, egg-laying and egg hatching, suggesting that *Period* may be implicated in the timing of mating behaviour, as well as in other components of daily temporal niche in Lepidoptera (Wang et al., 2023). The detection of a signal of positive selection on the Z-located gene *Period* in the genus *Morpho* could therefore be a consequence of the specialization into different ecological niches, as a result of reinforcement. It may also suggest a role for *Period* in the speciation process, by contributing to a pre-zygotic barrier.

Divergent evolution on the Z-chromosome in closely-related species

The observed faster evolution of genes located in the Z chromosome throughout the *Morpho* genus aligns with findings in other lepidoptera species as the Carolina sphinx moth (*Manduca sexta*), the

monarch (*Danaus plexippus*) or *Leptidea sinapis*, assessed using dN/dS ratios (Höök et al., 2023; Mongue et al., 2022). However, other studies in butterflies did not detect a faster Z-chromosome evolution. In the nymphalid species *Maniola jurtina* and *Pyronia tithonus*, transcriptomic data showed a slightly slower evolutionary rate on the Z-chromosome compared to autosomes (Rousselle et al., 2016). In the genus *Morpho*, we observed a higher evolutionary rate for genes located on the Z chromosome compared to those on the autosomes. This pattern was consistent both when analyzing all species together and in most of the pairwise comparisons between closely-related species. Nevertheless, no significant differences in evolutionary rates between autosomes and the Z chromosome were found in species pairs from distinct ecological niches, and the test for divergent evolutionary direction in the canopy *vs.* understory species did not reveal a more pronounced divergence in the Z-contigs genes as compared to the autosomal genes. In contrast, closely-related species pairs, and in particular species pairs with overlapping habitats and flight times, all showed a significantly different evolution between the Z and autosomal contigs.

Nevertheless, the contribution of different selection regimes acting on the Z chromosome *vs.* the autosomes to the variation in dN/dS observed in our study can not be fully estimated because of several limitations. The *Morpho* genomes studied here display a high level of heterozygosity, so that the substitutions observed between species are not necessarily fixed within species, and such intra-specific polymorphism might skew our estimation of dN/dS between closely-related species (Mugal et al., 2020). The difference in effective population sizes between the Z chromosome and the autosomes could thus partly explain the observed difference in dN/dS. Our analyses were also conducted on a subset of genes, specifically single-copy orthologs, identified through OrthoFinder and common across all genomes. This subset, representing genes found in all Lepidoptera, may exclude genes that are unique to the *Morpho* genus.

Interestingly, the significant differences in evolutionary rates between the Z-contig and autosomes appeared to be associated with the presence of big genomic inversions on the Z-contig. In *Manduca sexta*, an inversion of 1Mb in the chromosome Z seems to evolve under positive selection, driving the inversion to near fixation. This inversion is considered adaptive as it contains a significant excess of "unbiased genes" (genes expressed in both sexes) while the rest of the Z chromosome appears to have male-biased gene expression. As unbiased genes will be in hemizygous state in females, an inversion could be fixed if recessive beneficial mutations are exposed to selection (Mongue and Kawahara, 2022). The comparison of clade-specific analysis and pairwise analyses of dN/dS suggests that the acceleration divergence in Z-located genes as compared to the autosomes is particularly marked in closely-related species living in sympatry and exhibiting inversions. These findings are consistent with an effect of the Z-chromosome divergence, fueled by both chromosomal rearrangement and variation in protein sequences on the sex-chromosome in species divergence.

Conclusions

Altogether, our results evidence the accelerated evolution of the Z chromosome as compared to the autosomes throughout the butterfly genus *Morpho*, especially between closely-related species living in sympatry. Whether reproductive interferences between sympatric species fuel the accelerated evolution of this sex chromosome remains an open question. The potential role of the Z chromosome in pre and post zygotic barrier to gene flow needs to be investigated in further studies using sympatric and allopatric populations of different species.

Materials and Methods

The nuclear and mitochondrial assemblies of the genomes of *Morpho helenor*, *M. achilles* and *M. deidamia* were previously described in (Bastide et al., 2023). Here, we sequenced, assembled and annotated the whole genome of eight additional *Morpho* species: five understory species - *M. amathonte*, *M. menelaus*, *M. granadensis*, *M. eugenia* and *M. marcus* - and three canopy species - *M. rhetenor*, *M. hecuba* and *M. telemachus*. For this last species, two different morphs

co-exist in sympatry: males with blue/grey or golden wings, and we sequenced one individual of each morph.

Butterfly sampling

The male butterflies used for sequencing in this study were collected with handnets in Panama, Veraguas district (GPS coordinates: 8.525869707300163, -81.13020529212375) in July 2022 for *M. granadensis* and *M. amathonte* (Export permit number: PA-01-ARB-076-2022) and in French Guiana, Roura district (GPS coordinates: 4.5917807378071975, -52.20357910219149) in october 2022 for *M. eugenia, M. marcus, M. hecuba, M. telemachus* grey and gold morphs, *M. menelaus, M. rhetenor* (authorization number: R03-22-10-18-0001). The butterfly samples were then SNAP-frozen and kept at -80°C.

DNA extractions and genome sequencing

For genomic analyses, the DNA extraction was carried out from the thorax muscles using the Qiagen Genomic-tip 100/G kit, following supplier instructions. Library preparation and sequencing were performed according to the manufacturer's instructions "Procedure & Checklist – Preparing whole genome and metagenome libraries using SMRTbell® prep kit 3.0 ». At each step, DNA was quantified using the Qubit dsDNA HS Assay Kit (Life Technologies). DNA purity was tested using the nanodrop (Thermofisher) and size distribution and degradation assessed using the Femto pulse Genomic DNA 165 kb Kit (Agilent). Purification steps were performed using AMPure PB beads (PacBio) and SMRTbell cleanup beads (PacBio). For 9 samples, 5µg of DNA was purified then repaired using "SMRTbell Damage Repair Kit SPV3" (PacBio) and sheared between 15kb to 20 kb using the Megaruptor 1 system (Diagenode). For *Morpho amathonte*, *M. granadensis* and *M. telemachus* gold samples, a single library was prepared. For the other 6 samples, multiplex libraries were prepared using SMRTbell Barcoded Adaptater kit 8A for *M. hecuba*/*M. rhetenor*, *M. telemachus* grey/*M. marcus* and *M. eugenia*/*M. menelaus*. A nuclease treatment was performed on the 6 libraries folowed by a size selection step using a 6, 8 or 10kb cut off on the PippinHT Size Selection system (Sage Science) with "0.75% Agarose, 6-10 kb High Pass, 75E protocol". Using Binding kit 3.2 kit and sequencing kit 2.0, libraries were sequenced with the adaptive loading method onto 6 SMRTcells (+2 extra SMRTcells for *M. menelaus* sample) on Sequel2 instrument at 90 pM with a 2 hours pre- extension and a 30 hours movie.

Nuclear and mitochondrial genome assembly

Heterozygosity for each PacBio dataset was estimated with Jellyfish (v.2.3.0) (Marcais and Kingsford, 2011) (jellyfish count and hist options). The resulting histograms were visualized with GenomeScope online version 2.0 (Ranallo-Benavidez et al., 2020). Assemblies were performed using Hifiasm v0.19.5 (Cheng et al., 2021). Lepidoptera genomes are particularly heterozygous and high heterozygosity imposes a challenge for most genome assemblers as it may be difficult to make the distinction between different alleles at the same locus and paralogs at different loci. Raw assemblies from heterozygous genomes are thus expected to contain high levels of false duplications (Asalone et al., 2020). Hifiasm allows using different levels of purge to remove redundant contigs. We systematically produced assemblies using two different purge options: no purge and purge in the most aggressive way (options -l0 and -l3 respectively). For each assembly, we estimated basic statistics (number of contigs, size of contigs, N50) using the "stats.sh" program from the BBMap v38.93 package (Bushnell, 2014). We assessed the completeness of assemblies obtained with Hifiasm using the different options with BUSCO v5.2.2 and MetaEuk for gene prediction against the *lepidoptera_odb*10 database (Manni et al., 2021). In several cases, the BUSCO results showed a high level of duplications in the final assembly, even when using the aggressive mode in hifiasm. In these cases, we used Purge_dups v1.2.5 to remove false haplotypic duplications, and then we reassessed completeness using BUSCO. For every species, we chose the final assembly among the

different assemblies produced with or without the use of Purge_dups, based in the basic statistics and the BUSCO score. The mitochondrial genome for all *Morpho* species was assembled directly from the PacBio Hifi reads with Rebaler (https://github.com/rrwick/Rebaler) as described in (Bastide et al., 2023) and using the mitochondrial genome from *M. helenor* as a reference.

All sequences obtained in this study have been submitted to NCBI GenBank.

Genome annotation and identification of circadian genes

For each *Morpho* species, we created a *de novo* library of repetitive elements from each assembled genome with RepeatModeler v2.0.2a (Flynn et al., 2020) with the option -s (slow search). This library was then used with RepeatMasker 4.1.2.p1 (Flynn et al., 2020) to produce softmasked assemblies needed for the annotation.

Structural annotation was carried out with BRAKER v2.1.6 (Bruna et al., 2021; Hoff et al., 2016), using the *arthropoda_odb*10 protein data set from OrthoDB (Kriventseva et al., 2019). BRAKER2 *ab initio* gene predictions were performed with AUGUSTUS v3.4.0b (Buchfink et al., 2015) and GeneMark-EP+ v4.64 (Lomsadze et al., 2005) with two rounds of training. The resulting .gff files containing predicted genes were filtered to keep only the longest isoform and were screened to remove incomplete gene coding models (i.e. genes coding with start and/or stop codon missing in its cds) with AGAT (Dainat et al., 2020). The filtered .gff files produced were used in the following steps.

The functional annotation was added to the BRAKER2 predictions in two parts, first, we ran InterProScan v5.33-72.0 (Quevillon et al., 2005) on the files produced after two rounds of BRAKER2 using the option -f XML. Second, the XML file produced by InterProScan and the previously filtered .gff file were used in Funannotate v1.8.13 (Palmer and Stajich, 2016) with the option "annotate" to obtain a multi-fasta file of protein coding genes for each species. We followed this procedure on the nine new genomes assembled in this paper and on the three previously published genomes of *M. helenor*, *M. achilles* and *M. deidamia*, to obtain comparable annotations throughout the 12 genomes. To assess the quality of the gene-set predicted for each species, we ran BUSCO v5.2.2 analyses on the protein file generated BRAKER2 with selection of the protein mode and the *lepidoptera_odb*10 database. Finally, identification and removal of foreign sequences from annotations were performed using ContScout (Bálint et al., 2024)

We then specifically studied eight different genes known to be involved in the circadian clock in butterflies: *Clock, Cycle, Period, Timeless, Cry1, Cry2, Vrille* and *PDP1*). The position, the proteic and nucleotidic sequences of the genes were extracted from the final gff files produced at the annotation step.

Phylogenetic relationships between *Morpho* species

To infer the phylogenetic relationships between the 12 sequenced genomes of *Morpho* butterflies, we followed the procedure explained in (Wright et al., 2023). Single copy orthologs common to all 12 genomes were extracted using OrthoFinder v2.5.5 (Emms and Kelly, 2019). Orthologs were aligned using Mafft with default options (Katoh et al., 2002) and trimmed using trimAl (Capella-Gutiérrez et al., 2009). Trimmed alignments were concatenated to produce a phylip supermatrix with catfasta2phyml (https://github.com/nylander/catfasta2phyml). This matrix was used in IQ-TREE (Nguyen et al., 2015) to infer the species tree under the Q.mammal+F+I+R8 substitution model and ultrafast bootstrap with 1000 replicates (Hoang et al., 2018) based on the Bayesian Information Criterion (BIC) after ModelFinder analyses (Kalyaanamoorthy et al., 2017). The consensus tree was visualized using FigTree v1.4.4 (http://tree.bio.ed.ac.uk/software/figtree/). In addition, for the two individuals of *Morpho telemachus*, we aligned the OPacBio HiFi reads and called SNPs as for the ABBA-BABA analysis and computed a genome-wide dxy value using the scripts available at https://github.com/simonhmartin/genomics_general.

ABBA-BABA scans for introgression

To test for potential introgression events between the genomes of the sympatric species in the understory clade, we applied ABBA-BABA tests (Green et al., 2010). This test relies on a 4-species tree [(((P1,P2),P3),O)] to detect the site trees deviating from the expectation based on the species tree (*i.e.*, ABBA or BABA, whereas we should expect AABB or AAAB) (Martin et al., 2015). Thus, we first selected two species groups that could be tested under this framework: *Morpho achilles* (P1), *M. helenor* (P2), *M. granadensis* (P3), *M. deidamia* (outgroup). Then, we aligned the PacBio HiFi reads to one reference genome (*M. helenor*) using Minimap2 v.2.8 and we called SNPs using VarScan v2.4.6. The resulting VCF file was filtered keeping only biallelic snps and removing indels. Positions associated with a read depth lower than 15 or greater than 150, with general quality lower than 30 or with missing genotype in at least one sample were converted to missing. This filtered vcf was then phased using beagle v5.4 and processed to obtain the allelic frequencies per each site using the python script freq.py available at `https://github.com/simonhmartin`. D statistic was then computed using the scripts for ABBA BABA `https://github.com/simonhmartin` and plotted for each contig of the reference genome greater than 10 Mb. This threshold was chosen to avoid the comparison between contigs that differ too much in their size (and thus in the number of sites used to obtain the chromosome-wide D mean), and facilitate the comparison with the analysis performed with syri, presented in the following paragraph.

Identification of the Z contig, synteny and detection of chromosomal rearrangements between *Morpho* genomes

We have previously identified the contig corresponding to the Z chromosome for *Morpho helenor*, *M. achilles* and *M. deidamia*, by comparing the assemblies produced by Hifiasm to the genome of the species *Maniola jurtina*, as this species represents the closest relative *Morpho* for which a high-quality chromosome-level assembly is available (Bastide et al., 2023). Here, we used D-genies to pair-map the genome of *M. helenor* the newly assembled *Morpho* species genome (*M. rhetenor*, *M. hecuba*, *M. telemachus*, *M. amathonte*, *M. menelaus*, *M. granadensis*, *M. eugenia* and *M. marcus*) treating *M. helenor* genome as the target reference and the new *Morpho* species genome as the query. This alignment permitted us to visually find, for each species, the contig corresponding to the Z contig of *M. helenor*.

To study the synteny and major rearrangements all over the genome, we aligned the genomes of different species by pair, using the online version of D-genies (Cabanettes and Klopp, 2018). Given our focus on synteny among closely related species, we conducted comparisons involving all species within the "Canopy" clade. Specifically, three comparisons were performed: *Morpho hecuba* vs *M. telemachus* blue, *M. telemachus* blue vs *M. telemachus* gold, and *M. telemachus* gold vs *M. rhetenor*. For the "Understory" clade, we also performed comparisons between close species: *M. amathonte* vs *M. menelaus*, *M. granadensis* vs *M. helenor* and *M. helenor* vs. *M. achilles*. Finally, we added the paired analysis of the two basal sister species: *M. eugenia* vs *M. marcus*. Paired alignments were performed using the Minimap2 aligner. (Li, 2018) in D-genies (see Fig. S3). To facilitate cross-species whole-genome comparisons, we standardized the assemblies by filtering out contigs smaller than 10 Mb, retaining approximately 90% of the total genome content for most species. However, in the case of *M. hecuba*, this threshold only covered 77% of the genome. Therefore, for this species, we adjusted the threshold to retain contigs larger than 5 Mb, ensuring coverage of 90% of the genome. Since we were particularly interested in genomic inversions, we visualy inspected the paired analyses produced by D-genies contig by contig. For any contig pair in which inversions were detected, we conducted additional analysis using SyRI, as this tool provides information on the size of each inversion. We were unable to conduct whole-genome comparisons with SyRI due to its requirement for the two genomes to be homologous and have matching contig names, typically necessitating chromosome-level assemblies. Since our assemblies lacked chromosome-level resolution and varied in contig number and nomenclature, we only used SyRI for contig-by-contig comparisons. Paired comparisons followed the methodology described in (Bastide

et al., 2023). Briefly, paired alignments of the equivalent contigs were generated using Minimap2, and the resulting SAM files were analyzed with SyRI to detect inversions (Goel et al., 2019). The genomic structures predicted by SyRI were visually represented using plotsr (Goel and Schneeberger, 2022).

Detection of positive selection in circadian genes and throughout the whole genome

To explore the genetic basis of the divergence in temporal niches, we searched for signature of selection in eight circadian genes (*Clock, Cycle, Period, Timeless, Cry1, Cry2, Vrille* and *PDP1*). We first generated trees for each gene with IQ-TREE (Nguyen et al., 2015) and ModelFinder. These trees were then used in the Codeml program in the PAML package (version 4.8) (Álvarez-Carretero et al., 2023; Yang et al., 1997) to detect signals of positive selection. PAML estimates the omega ratio (c) using maximum likelihood. The omega ratio compares non-synonymous (dN) against synonymous (dS) substitutions per site. We used random site models to test for positive selection at the codon scale on the genes. Branch site models were also computed to estimate selective pressures at codon sites within different lineages. Three types of hypotheses were tested under the PAML branch site model: (1) we searched for differences of positive selection on the branch leading to the two most basal *Morpho* species: *M.marcus* and *M.eugenia vs.* as this clade was the earliest diverging clade in the genus around 28MYA (Chazot et al., 2021). We labeled these two species as foreground branches and the rest of the species as background branches; (2) as the evolution of circadian genes might be linked to differences in the amount of light available, we looked for traces of positive selection on the lineages of the *Morpho* species living in the canopy *vs* the understory; and (3) because time activity is expected to be influenced by circadian genes, we looked for evidence of positive selection in the species where males display an early flight activity (patrolling from 6:00 to 10:00 am) *vs* a late flight activity (patrolling after 10:00 am). All models were always compared to a null model, assuming an omega ratio of 1 for all sites and across all lineages. To determine significance, the null model and the positive selection model were compared using a likelihood ratio test (LRT) following a Chi2 distribution, and Bayes Empirical Bayes (BEB) analyses were run to identify the positively selected amino acids (Álvarez-Carretero et al., 2023; Yang et al., 1997). All the analyses were carried out using PAMLX (Xu and Yang, 2013)

To identify selective regimes acting on genes located on the autosomes *vs.* the Z contig, we partitioned the genome of each species into two distinct segments: autosomal contigs and the Z contig. Subsequently, we applied the annotation procedure outlined in the "Genome Annotation" section to retrieve the CDS-transcript sequences predicted by Funannotate for each genomic partition. Next, we extracted single-copy orthologs shared across all 12 genomes using OrthoFinder v2.5.5.148 genes and 8209 genes were retrieved from the Z contig and the autosomes respectively. DNA sequences were translated into an amino acid sequences using Seqkit v2.1.0 (Shen et al., 2016) and amino acid sequences were aligned using Mafft. Finally, we used PAL2NAL for the correction of the nucleotide sequences using the corresponding aligned protein sequences Suyama et al., 2006.

Then, we used the one-ratio model implemented in PAML to calculate the dN/dS ratio (also called omega ω) on all the orthologs found on the Z contig and on the autosomal contigs. We measured the w ratio of those orthologs separately. Because large gaps in gene alignments can cause the dN/dS to artificially increase when an ortholog is highly different in between species, we also measured the ω ratio of *Morphos* orthologs on gapless alignments. We used non-parametric Wilcoxon statistics to test whether the ω ratio measured on the orthologs found on the Z contig was higher than the ω ratio measured on the orthologs found on the autosomal contigs. To account for the unequal group sizes in the number of genes found on the autosomes and the Z contig, we performed a permutation test. We randomly drew 148 autosomal genes from the pool of 8209 autosomal genes and compared their mean ω ratio to the mean ω ratio of the 148 Z genes. This procedure was repeated 1000 times for both the gapless and the raw dataset.

To investigate whether the evolution of autosomes and the Z chromosome differs were linked to divergent evolution in the different ecological niches, we conducted the following analyses: First, we

compared the evolutionary rates of genes located on the Z chromosome between species from the canopy and those from the understory, and we did the same for genes located on autosomes. Our goal was to identify the proportion of genes, either on autosomes or the Z chromosome, that show significant differences in evolutionary rates between the canopy and understory clades. To assess these differences, we used the Clade model in codeml ($Model = 3$, $NSsites = 2$), which employs the likelihood ratio test (LRT) to detect genes with significant rate variations between clades. We then compared whether the proportion of genes with significant differences between clades was higher for genes on the autosomes or the Z chromosome. This comparison was made using a Z-test for proportions, which accounts for the large difference in the number of genes between the two groups. Second, to investigate whether evolutionary rates differ between autosomes and the Z chromosome within each clade (canopy or understory) and to understand the potential role of these genomic regions in adaptation to the ecological niche, we analyzed species separately within each clade, allowing to include orthologous genes shared within clades but absent from the alternative. These clade-specific genes could play a significant role in adaptation to the difference niches. For each clade, we thus identified single-copy orthologous genes located on the autosomes and the Z chromosome and used the M0 model in codeml to calculate the dN/dS ratio for these gene sets. For the canopy clade, we identified 11,200 autosomal orthologs and 354 Z-linked orthologs that were common to the three species studied (*M. rhetenor*, *M. hecuba*, and *M. telemachus*). For the eight species from the understory, we identified 9,299 autosomal single-copy orthologs and 189 Z-linked orthologs. With this approach, we were expecting to recover genes that may play specific roles in adaptation to particular ecological niches, which might have been overlooked in our previous analyses that included species from different niches. Finally, we used a non-parametric Wilcoxon permutation test to compare the dN/dS ratios between groups.

To test whether the differences in the dN/dS ratio between autosomes and the Z chromosome stemmed mostly from divergence in specific species pairs, we estimated the substitution rates for genes in each genomic region using pairwise analyses with the YN00 program from PAML. Orthologous genes used in the genus-wide analysis were realigned by pair and used in the YN00 analysis with the method of Yang and Nielsen (Yang and Nielsen, 2000). We conducted comparisons between pairs of closely related species within the same niche, as well as between species from distinct niches. Specifically, 11 paired comparisons were made: two pairs from the canopy, six pairs from the understory (paired close species living in sympatry or allopatry), the two species from the basal clade, and two comparisons between one canopy and one understory species. To assess differences in ω values between autosomes and the Z chromosome for each species pair, we used a non-parametric Wilcoxon test, followed by a permutation test.

Data Availability Statement

The raw sequencing data and final genome assemblies generated in this study have been submitted to the NCBI BioProject database under accession numbers PRJNA1069011 (for raw fastq files) and PRJNA1063620 (for final assemblies of the new genomes sequenced here).

Acknowledgments

We thank Jean-Philippe Vernadet for help with scripts. We thank Louis Duchemin and Stefano Mona for discussions on previous versions of this paper. All the analyses and simulations were performed on the Plateforme de Calcul Intensif et Algorithmique PCIA (Muséum national d'histoire naturelle, Centre national de la recherche scientifique), the MeSU platform at Sorbonne-Université, the Genotoul bioinformatics platform Toulouse Occitanie (Bioinfo Genotoul, https://doi.org/10.15454/1.5572369328961167E12) and the GenOuest bioinformatics core facility (https://www.genouest.org). This work was funded by the European Union (ERC Consolidator grant OUTOFTHEBLUE, project number 101088089). Views and opinions expressed are however

those of the authors only and do not necessarily reflect those of the European Union or the European Research Council. Neither the European Union nor the granting authority can be held responsible for them.

References

Álvarez-Carretero, S., Kapli, P., and Yang, Z. (2023). Beginner's guide on the use of paml to detect positive selection. *Molecular Biology and Evolution*, 40(4):msad041.

Asalone, K. C., Ryan, K. M., Yamadi, M., Cohen, A. L., Farmer, W. G., George, D. J., Joppert, C., Kim, K., Mughal, M. F., Said, R., Toksoz-Exley, M., Bisk, E., and Bracht, J. R. (2020). Regional sequence expansion or collapse in heterozygous genome assemblies. *PLoS Computational Biology*, 16(7).

Bálint, B., Merényi, Z., Hegedüs, B., Grigoriev, I. V., Hou, Z., Földi, C., and Nagy, L. G. (2024). Contscout: sensitive detection and removal of contamination from annotated genomes. *Nature Communications*, 15(1):936.

Bastide, H., López-Villavicencio, M., Ogereau, D., Lledo, J., Dutrillaux, A.-M., Debat, V., and Llaurens, V. (2023). Genome assembly of 3 Amazonian Morpho butterfly species reveals Z-chromosome rearrangements between closely related species living in sympatry. *GigaScience*, 12:giad033.

Blandin, P. and Purser, B. (2013). Evolution and diversification of neotropical butterflies: Insights from the biogeography and phylogeny of the genus morpho fabricius, 1807 (nymphalidae: Morphinae), with a review of the geodynamics of south aamerica. *Tropical Lepidoptera Research*, pages 62–85.

Brady, D., Saviane, A., Cappellozza, S., and Sandrelli, F. (2021). The circadian clock in lepidoptera. *Frontiers in Physiology*, 12:776826.

Bruna, T., Hoff, K. J., Lomsadze, A., Stanke, M., and Borodovsky, M. (2021). Braker2: automatic eukaryotic genome annotation with genemark-ep plus and augustus supported by a protein database. *NAR Genomics and Bioinformatics*, 3(1).

Buchfink, B., Xie, C., and Huson, D. H. (2015). Fast and sensitive protein alignment using diamond. *Nature methods*, 12(1):59–60.

Bushnell, B. (2014). Bbmap: A fast, accurate, splice-aware aligner.[www document]. *URL https://www. osti. gov/se rvlets/purl/1241166*.

Cabanettes, F. and Klopp, C. (2018). D-genies: dot plot large genomes in an interactive, efficient and simple way. *PeerJ*, 6:e4958.

Capella-Gutiérrez, S., Silla-Martínez, J. M., and Gabaldón, T. (2009). trimal: a tool for automated alignment trimming in large-scale phylogenetic analyses. *Bioinformatics*, 25(15):1972–1973.

Charlesworth, B., Coyne, J. A., and Barton, N. H. (1987). The relative rates of evolution of sex chromosomes and autosomes. *The American Naturalist*, 130(1):113–146.

Chazot, N., Blandin, P., Debat, V., Elias, M., and Condamine, F. L. (2021). Punctuational ecological changes rather than global factors drive species diversification and the evolution of wing phenotypes in morpho butterflies. *Journal of Evolutionary Biology*, 34(10):1592–1607.

Chazot, N., Panara, S., Zilbermann, N., Blandin, P., Le Poul, Y., Cornette, R., Elias, M., and Debat, V. (2016). Morpho morphometrics: shared ancestry and selection drive the evolution of wing size and shape in *morpho* butterflies. *Evolution*, 70(1):181–194.

Cheng, H., Concepcion, G. T., Feng, X., Zhang, H., and Li, H. (2021). Haplotype-resolved de novo assembly using phased assembly graphs with hifiasm. *Nature Methods*, 18(2):170+.

Connallon, T., Olito, C., Dutoit, L., Papoli, H., Ruzicka, F., and Yong, L. (2018). Local adaptation and the evolution of inversions on sex chromosomes and autosomes. *Philosophical Transactions of the Royal Society B: Biological Sciences*, 373(1757):20170423.

Dainat, J., Hereñú, D., and Pucholt, P. (2020). Agat: Another gff analysis toolkit to handle annotations in any gtf/gff format. *Version v0*, 4:10–5281.

Devries, P. J., Austin, G. T., and Martin, N. H. (2008). Diel activity and reproductive isolation in a diverse assemblage of neotropical skippers (lepidoptera: Hesperiidae). *Biological Journal of the Linnean Society*, 94(4):723–736.

Emms, D. M. and Kelly, S. (2019). Orthofinder: phylogenetic orthology inference for comparative genomics. *Genome biology*, 20:1–14.

Ficarrotta, V., Hanly, J. J., Loh, L. S., Francescutti, C. M., Ren, A., Tunström, K., Wheat, C. W., Porter, A. H., Counterman, B. A., and Martin, A. (2022). A genetic switch for male uv iridescence in an incipient species pair of sulphur butterflies. *Proceedings of the National Academy of Sciences*, 119(3):e2109255118.

Flynn, J. M., Hubley, R., Goubert, C., Rosen, J., Clark, A. G., Feschotte, C., and Smit, A. F. (2020). Repeatmodeler2 for automated genomic discovery of transposable element families. *Proceedings of the National Academy of Sciences*, 117(17):9451–9457.

Fraïsse, C. and Sachdeva, H. (2021). The rates of introgression and barriers to genetic exchange between hybridizing species: sex chromosomes vs autosomes. *Genetics*, 217(2):iyaa025.

Gayman, J.-M., Merlier, F., Ouvaroff, J., Bénéluz, F., Lacomme, D., Purser, B., and Berthier, S. (2016). *Les Morpho: distribution, diversification, comportement*. Association des lépidoptéristes de France.

Goel, M. and Schneeberger, K. (2022). plotsr: visualizing structural similarities and rearrangements between multiple genomes. *Bioinformatics*, 38(10):2922–2926.

Goel, M., Sun, H., Jiao, W.-B., and Schneeberger, K. (2019). Syri: finding genomic rearrangements and local sequence differences from whole-genome assemblies. *Genome biology*, 20(1):1–13.

Gotter, A. L., Levine, J. D., and Reppert, S. M. (1999). Sex-linked period genes in the silkmoth, antheraea pernyi: implications for circadian clock regulation and the evolution of sex chromosomes. *Neuron*, 24(4):953–965.

Green, R. E., Krause, J., Briggs, A. W., Maricic, T., Stenzel, U., Kircher, M., Patterson, N., Li, H., Zhai, W., Fritz, M. H.-Y., et al. (2010). A draft sequence of the neandertal genome. *science*, 328(5979):710–722.

Hänniger, S., Dumas, P., Schöfl, G., Gebauer-Jung, S., Vogel, H., Unbehend, M., Heckel, D. G., and Groot, A. T. (2017). Genetic basis of allochronic differentiation in the fall armyworm. *BMC evolutionary biology*, 17:1–14.

Hoang, D. T., Chernomor, O., Von Haeseler, A., Minh, B. Q., and Vinh, L. S. (2018). Ufboot2: improving the ultrafast bootstrap approximation. *Molecular biology and evolution*, 35(2):518–522.

Hoff, K. J., Lange, S., Lomsadze, A., Borodovsky, M., and Stanke, M. (2016). Braker1: Unsupervised rna-seq-based genome annotation with genemark-et and augustus. *Bioinformatics*, 32(5):767–769.

Höök, L., Vila, R., Wiklund, C., and Backström, N. (2023). Temporal dynamics of faster neo-z evolution in butterflies. *bioRxiv*.

Hooper, D. M. and Price, T. D. (2017). Chromosomal inversion differences correlate with range overlap in passerine birds. *Nature ecology & evolution*, 1(10):1526–1534.

Iiams, S. E., Lugena, A. B., Zhang, Y., Hayden, A. N., and Merlin, C. (2019). Photoperiodic and clock regulation of the vitamin a pathway in the brain mediates seasonal responsiveness in the monarch butterfly. *Proceedings of the National Academy of Sciences*, 116(50):25214–25221.

Irwin, D. E. (2018). Sex chromosomes and speciation in birds and other zw systems. *Molecular Ecology*, 27(19):3831–3851.

Johnson, N. A. and Lachance, J. (2012). The genetics of sex chromosomes: evolution and implications for hybrid incompatibility. *Annals of the New York Academy of Sciences*, 1256(1):E1–E22.

Kalyaanamoorthy, S., Minh, B. Q., Wong, T. K., Von Haeseler, A., and Jermiin, L. S. (2017). Modelfinder: fast model selection for accurate phylogenetic estimates. *Nature methods*, 14(6):587–589.

Katoh, K., Misawa, K., Kuma, K.-i., and Miyata, T. (2002). Mafft: a novel method for rapid multiple sequence alignment based on fast fourier transform. *Nucleic acids research*, 30(14):3059–3066.

Kriventseva, E. V., Kuznetsov, D., Tegenfeldt, F., Manni, M., Dias, R., Simao, F. A., and Zdobnov, E. M. (2019). Orthodb v10: sampling the diversity of animal, plant, fungal, protist, bacterial and viral genomes for evolutionary and functional annotations of orthologs. *Nucleic Acids Research*, 47(D1):D807–D811.

Le Roy, C., Amadori, D., Charberet, S., Windt, J., Muijres, F. T., Llaurens, V., and Debat, V. (2021a). Adaptive evolution of flight in morpho butterflies. *Science*, 374(6571):1158–1162.

Le Roy, C., Roux, C., Authier, E., Parrinello, H., Bastide, H., Debat, V., and Llaurens, V. (2021b). Convergent morphology and divergent phenology promote the coexistence of morpho butterfly species. *Nature communications*, 12(1):7248.

Li, H. (2018). Minimap2: pairwise alignment for nucleotide sequences. *Bioinformatics*, 34(18):3094–3100.

Lohse, K., Weir, J., of Life, W. S. I. T., of Life Consortium, D. T., et al. (2021). The genome sequence of the meadow brown, maniola jurtina (linnaeus, 1758). *Wellcome Open Research*, 6.

Lomsadze, A., Ter-Hovhannisyan, V., Chernoff, Y., and Borodovsky, M. (2005). Gene identification in novel eukaryotic genomes by self-training algorithm. *Nucleic Acids Research*, 33(20):6494–6506.

Mank, J. E., Nam, K., and Ellegren, H. (2009). Faster-z evolution is predominantly due to genetic drift. *Molecular biology and evolution*, 27(3):661–670.

Manni, M., Berkeley, M. R., Seppey, M., Simao, F. A., and Zdobnov, E. M. (2021). Busco update: Novel and streamlined workflows along with broader and deeper phylogenetic coverage for scoring of eukaryotic, prokaryotic, and viral genomes. *Molecular Biology and Evolution*, 38(10):4647–4654.

Marcais, G. and Kingsford, C. (2011). A fast, lock-free approach for efficient parallel counting of occurrences of k-mers. *Bioinformatics*, 27(6):764–770.

Martin, S. H., Dasmahapatra, K. K., Nadeau, N. J., Salazar, C., Walters, J. R., Simpson, F., Blaxter, M., Manica, A., Mallet, J., and Jiggins, C. D. (2013). Genome-wide evidence for speciation with gene flow in heliconius butterflies. *Genome research*, 23(11):1817–1828.

Martin, S. H., Davey, J. W., and Jiggins, C. D. (2015). Evaluating the use of abba–baba statistics to locate introgressed loci. *Molecular biology and evolution*, 32(1):244–257.

Meisel, R. P. and Connallon, T. (2013). The faster-x effect: integrating theory and data. *Trends in genetics*, 29(9):537–544.

Merlin, C. and Reppert, S. M. (2009). Lepidopteran circadian clocks. *Molecular Biology and Genetics of the Lepidoptera*, page 137.

Miyatake, T., Matsumoto, A., Matsuyama, T., Ueda, H. R., Toyosato, T., and Tanimura, T. (2002). The period gene and allochronic reproductive isolation in bactrocera cucurbitae. *Proceedings of the Royal Society of London. Series B: Biological Sciences*, 269(1508):2467–2472.

Mongue, A. J. and Baird, R. B. (2023). Genetic drift drives faster-z evolution in the salmon louse lepeophtheirus salmonis. *bioRxiv*.

Mongue, A. J., Hansen, M. E., and Walters, J. R. (2022). Support for faster and more adaptive z chromosome evolution in two divergent lepidopteran lineages. *Evolution*, 76(2):332–345.

Mongue, A. J. and Kawahara, A. Y. (2022). Population differentiation and structural variation in the manduca sexta genome across the united states. *G3*, 12(5):jkac047.

Mugal, C. F., Kutschera, V. E., Botero-Castro, F., Wolf, J. B., and Kaj, I. (2020). Polymorphism data assist estimation of the nonsynonymous over synonymous fixation rate ratio ω for closely related species. *Molecular biology and evolution*, 37(1):260–279.

Nguyen, L.-T., Schmidt, H. A., Von Haeseler, A., and Minh, B. Q. (2015). Iq-tree: a fast and effective stochastic algorithm for estimating maximum-likelihood phylogenies. *Molecular biology and evolution*, 32(1):268–274.

Noor, M. A., Grams, K. L., Bertucci, L. A., and Reiland, J. (2001). Chromosomal inversions and the reproductive isolation of species. *Proceedings of the National Academy of Sciences*, 98(21):12084–12088.

Palmer, J. and Stajich, J. (2016). Funannotate: a fungal genome annotation and comparative genomics pipeline (v1. 5.2). *Zenodo doi*, 105281.

Payseur, B. A., Presgraves, D. C., and Filatov, D. A. (2018). Sex chromosomes and speciation. *Molecular ecology*, 27(19):3745.

Quevillon, E., Silventoinen, V., Pillai, S., Harte, N., Mulder, N., Apweiler, R., and Lopez, R. (2005). Interproscan: protein domains identifier. *Nucleic Acids Research*, 33(2):W116–W120.

Ranallo-Benavidez, T. R., Jaron, K. S., and Schatz, M. C. (2020). Genomescope 2.0 and smudgeplot for reference-free profiling of polyploid genomes. *Nature Communications*, 11(1).

Reppert, S. M. (2006). A colorful model of the circadian clock. *Cell*, 124(2):233–236.

Rousselle, M., Faivre, N., Ballenghien, M., Galtier, N., and Nabholz, B. (2016). Hemizygosity enhances purifying selection: lack of fast-z evolution in two satyrine butterflies. *Genome biology and evolution*, 8(10):3108–3119.

Saccheri, I. J., of Life, W. S. I. T., of Life Consortium, D. T., et al. (2023). The genome sequence of the squinting bush brown, bicyclus anynana (butler, 1879). *Wellcome open research*, 8.

Sackton, T. B., Corbett-Detig, R. B., Nagaraju, J., Vaishna, L., Arunkumar, K. P., and Hartl, D. L. (2014). Positive selection drives faster-z evolution in silkmoths. *Evolution*, 68(8):2331–2342.

Sæther, S. A., Sætre, G.-P., Borge, T., Wiley, C., Svedin, N., Andersson, G., Veen, T., Haavie, J., Servedio, M. R., Bures, S., et al. (2007). Sex chromosome-linked species recognition and evolution of reproductive isolation in flycatchers. *science*, 318(5847):95–97.

Sandrelli, F., Costa, R., Kyriacou, C. P., and Rosato, E. (2008). Comparative analysis of circadian clock genes in insects. *Insect molecular biology*, 17(5):447–463.

Schilthuizen, M., Giesbers, M., and Beukeboom, L. (2011). Haldane's rule in the 21st century. *Heredity*, 107(2):95–102.

Shen, W., Le, S., Li, Y., and Hu, F. (2016). Seqkit: a cross-platform and ultrafast toolkit for fasta/q file manipulation. *PloS one*, 11(10):e0163962.

Suyama, M., Torrents, D., and Bork, P. (2006). Pal2nal: robust conversion of protein sequence alignments into the corresponding codon alignments. *Nucleic acids research*, 34(suppl_2):W609–W612.

Swaegers, J., Sánchez-Guillén, R. A., Chauhan, P., Wellenreuther, M., and Hansson, B. (2022). Restricted x chromosome introgression and support for haldane's rule in hybridizing damselflies. *Proceedings of the Royal Society B*, 289(1979):20220968.

Tauber, E., Roe, H., Costa, R., Hennessy, J. M., and Kyriacou, C. P. (2003). Temporal mating isolation driven by a behavioral gene in drosophila. *Current Biology*, 13(2):140–145.

Taylor, R. S. and Friesen, V. L. (2017). The role of allochrony in speciation. *Molecular Ecology*, 26(13):3330–3342.

Tunstrom, K., Wheat, C. W., Parmesan, C., Singer, M. C., and Mikheyev, A. S. (2022). A genome for edith's checkerspot butterfly: An insect with complex host-adaptive suites and rapid evolutionary responses to environmental changes. *Genome Biology and Evolution*, 14(8):evac113.

Vicoso, B. and Charlesworth, B. (2006). Evolution on the x chromosome: unusual patterns and processes. *Nature Reviews Genetics*, 7(8):645–653.

Vicoso, B., Emerson, J., Zektser, Y., Mahajan, S., and Bachtrog, D. (2013). Comparative sex chromosome genomics in snakes: differentiation, evolutionary strata, and lack of global dosage compensation. *PLoS biology*, 11(8):e1001643.

Wadsworth, C., Li, X., and Dopman, E. (2015). A recombination suppressor contributes to ecological speciation in ostrinia moths. *Heredity*, 114(6):593–600.

Wang, D., Chen, J., Yuan, Y., Yu, L., Yang, G., and Chen, W. (2023). Crispr/cas9-mediated knockout of period reveals its function in the circadian rhythms of the diamondback moth plutella xylostella. *Insect Science*, 30(3):637–649.

Wright, A. E., Harrison, P. W., Zimmer, F., Montgomery, S. H., Pointer, M. A., and Mank, J. E. (2015). Variation in promiscuity and sexual selection drives avian rate of faster-z evolution. *Molecular ecology*, 24(6):1218–1235.

Wright, C. J., Stevens, L., Mackintosh, A., Lawniczak, M., and Blaxter, M. (2023). Chromosome evolution in lepidoptera. *bioRxiv*, pages 2023–05.

Xu, B. and Yang, Z. (2013). Pamlx: a graphical user interface for paml. *Molecular biology and evolution*, 30(12):2723–2724.

Yang, Z. et al. (1997). Paml: a program package for phylogenetic analysis by maximum likelihood. *Computer applications in the biosciences*, 13(5):555–556.

Yang, Z. and Nielsen, R. (2000). Estimating synonymous and nonsynonymous substitution rates under realistic evolutionary models. *Molecular biology and evolution*, 17(1):32–43.

Supporting Information

Table S1. Haploid size, heterozygosity estimated by GenomeScope and number of contigs covering 90% of the genome after cleaning the assemblies for *Morpho* species.

Species	Max heterozygosity (%)	Haploid size (Mb)	Number of contigs after assembly cleaning
M. helenor	3.34	356.25	25
M. achilles	2.78	363.68	26
M. deidamia	1.68	380.89	27
M. rhetenor	2.51	348.28	21
M. hecuba	1.72	406.52	32
M. amathonte	1.69	411.77	27
M. menelaus	3.38	384.59	26
M. granadensis	1.01	396.42	26
M. eugenia	2.54	441.88	23
M. marcus	2.34	397.67	23
M. telemachus gold	1.19	396.77	30
M. telemachus blue	1.11	404.21	26

Table S2. Contig name and size of the contig Z in different *Morpho* species. This contig was first identified by comparative analysis between the *Morpho helenor* genome and the well-assembled chromosome-level genome of *Maniola jurtina*. For the other *Morpho* species, we retrieved the Z contig by comparing their assemblies to that of *M. helenor*.

Species	Contig	Size (Mb)
M. helenor	ptg000030l	22.58
M. achilles	ptg000022l	24.85
M. deidamia	ptg000019l	22.52
M. rhetenor	ptg000004l	19.51
M. hecuba	ptg000050l	22.28
M. amathonte	ptg000018l	20.95
M. menelaus	ptg000017l	18.99
M. granadensis	ptg000001l	24.23
M. eugenia	ptg000031l	22.91
M. marcus	ptg000008l	21.43
M. telemachus gold	ptg000006l	25.06
M. telemachus blue	ptg000022l	25.00

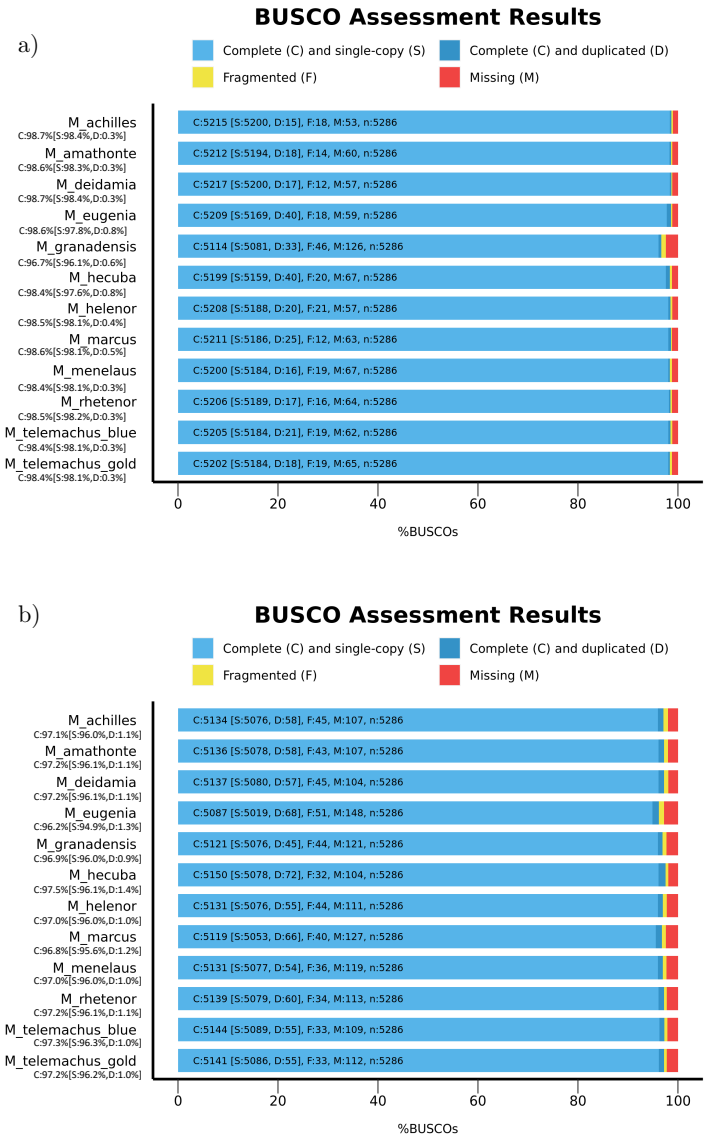

Figure S1. BUSCO scores of Complete BUSCOs (C), Complete and single-copy BUSCOs (S) Complete and duplicated BUSCOs (D), Fragmented BUSCOs (F), Missing BUSCOs (M) for a) complete assemblies produce by Hifiasm and Purge_dups (when needed) using genome mode and b) annotations generated by BRAKER2 in protein mode of 12 *Morpho* individuals. Notice that BUSCO assembly scores for *Morpho helenor*, *M. achilles* and *M. deidamia* have already been published in (Bastide et al., 2023).

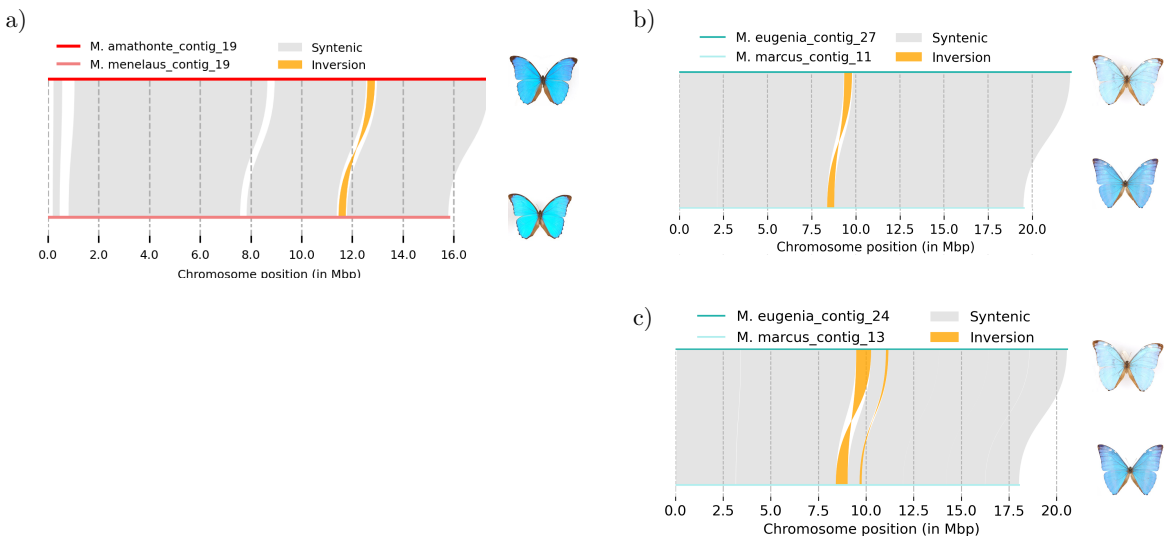

Figure S2. Paired comparisons of autosomes where inversions were detected between close *Morpho* species a) Contig ptg000019l for *M. amathonte* and *M. menelaus* b) contig ptg000027l of *M. eugenia* and the corresponding contig for *M. marcus* (ptg000011l) c) contig ptg000024l of *M. eugenia* and the corresponding contig for *M. marcus* (ptg000013l). Inversions are visible in dark yellow and syntenic regions in light gray.

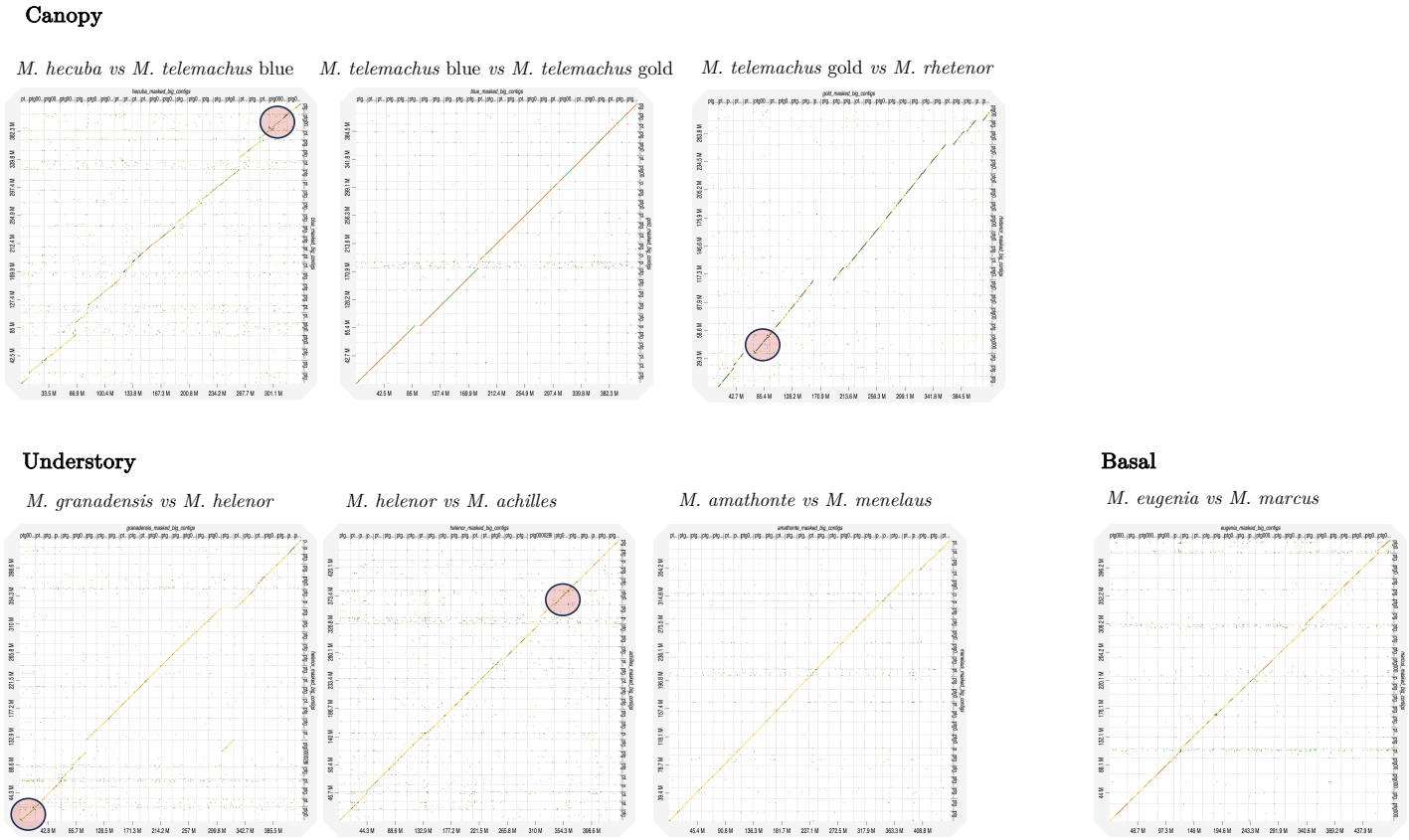

Figure S3. Paired whole-genome comparisons among closely related species of the genus *Morpho* belonging to three distinct clades: canopy, understory and basal. Genome assemblies were cleaned to retain only contigs of more than 10Mb (or 5Mb in the case of *M. hecuba*) to facilitate visualization. Detected genomic inversions in the contig Z were highlighted with red circles for ease of identification

Figures/omega_raw_data.pdf

Figure S4. Comparison of the *dN/dS* values measured for the 8357 genes located in either the autosomal contigs (in white) or the contig Z (in blue). The ω ratio values were computed using the one-ratio model implemented in PAML on raw ortholog alignments, and are represented in logarithmic scale.

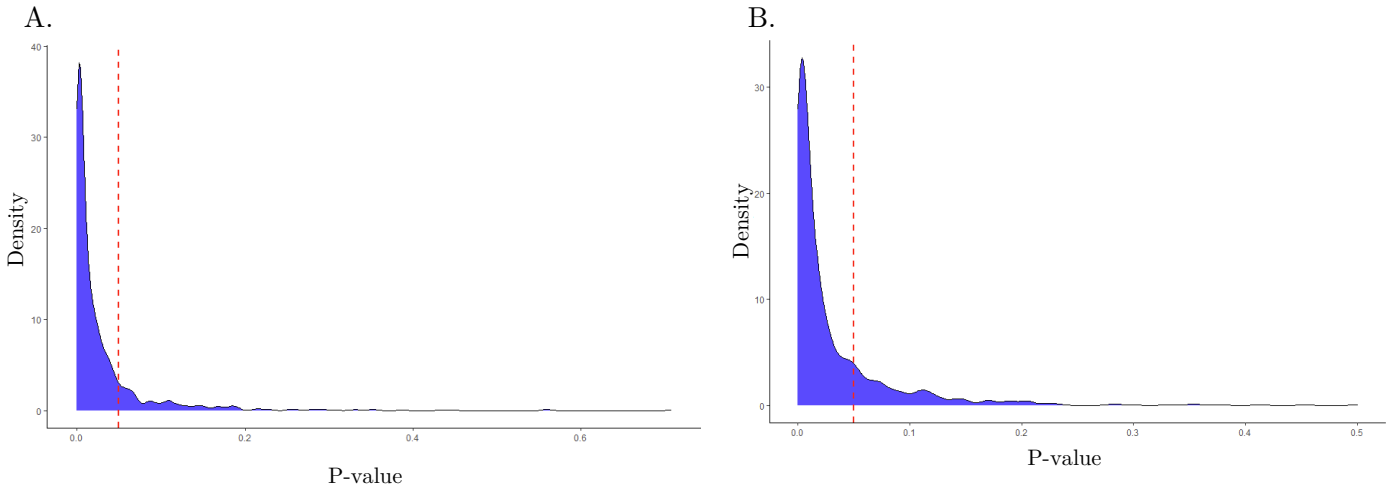

Figure S5. Permutation test to compare the mean ω ratio for autosomal genes and genes located on the Z contig. We randomly drew 148 autosomal genes from the pool of 8209 autosomal genes and compared their mean ω ratio to the mean ω ratio of the 148 genes located in the Z contig. This operation was repeated 1000 times. The distribution of p-values obtained from replicating Wilcoxon tests on the gapless alignment ω data is shown in (A), and the distribution of p-values obtained from replicating Wilcoxon tests on the raw alignment ω data is shown in (B). The red dotted line indicates the 0.05 p-value threshold.

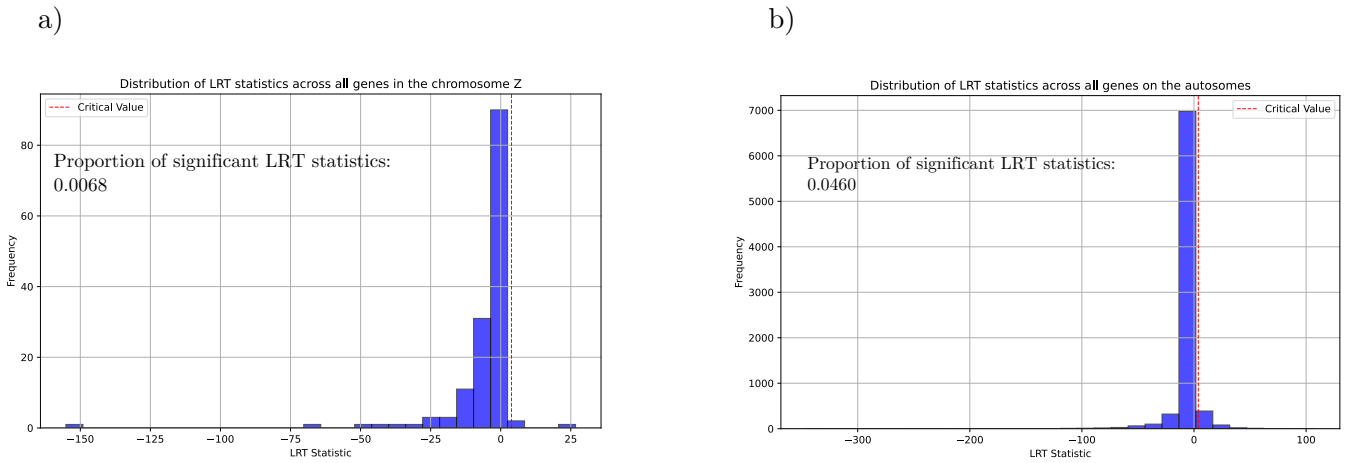

Figure S6. Likelihood ratio test (LRT) for a clade model on a) genes of the chromosome Z and b) genes located on the autosomes to compare canopy and understory species

Table S3. Number of genes predicted for the different *Morpho* species using BRAKER2 and Funannotate followed by the identification and removal of foreign sequences using ContScout (see text for details)

Species	Number of genes estimated	Number of genes after ContScout
M. helenor	29734	19860
M. achilles	21017	21017
M. deidamia	18620	18620
M. rhetenor	18350	18274
M. hecuba	20125	19289
M. amathonte	20345	20022
M. menelaus	19450	19450
M. granadensis	18454	18454
M. eugenia	20057	20057
M. marcus	19239	18705
M. telemachus gold	18300	18289
M. telemachus blue	18159	18139

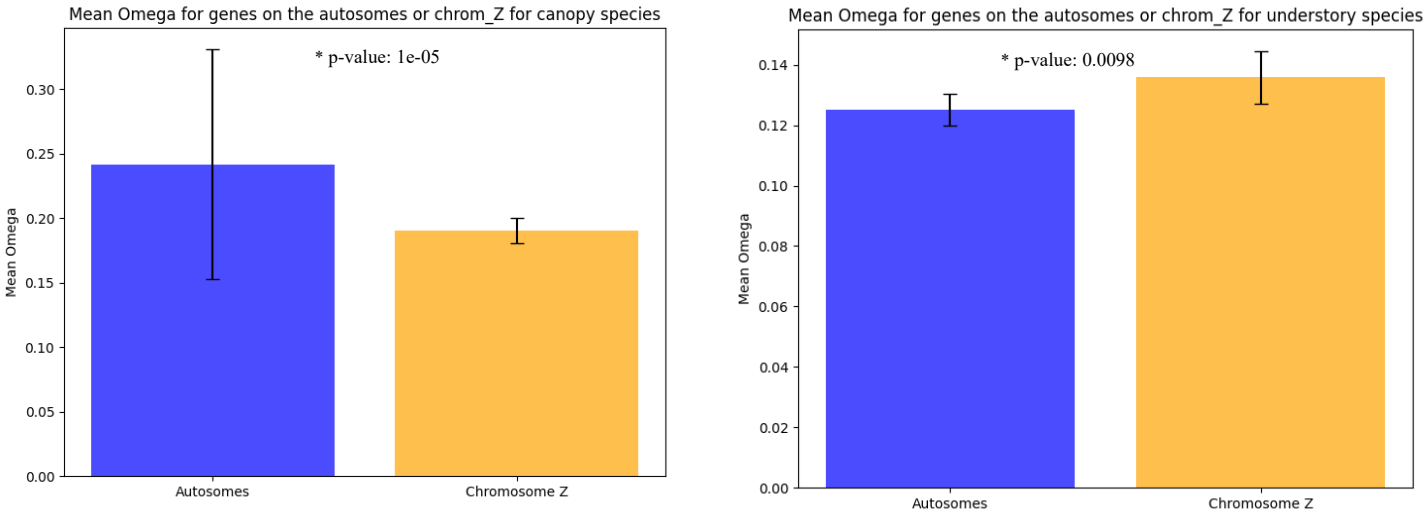

Figure S7. Permutation test to compare the mean ω ratio for autosomal genes and genes located on the Z chromosome within ecological niches (canopy or understory). ω values and p-values obtained from replicating Wilcoxon tests on each group are shown in left) species from the canopy and right) species from the understory